Active–passive pulse laser based on gold nanobipyramids at 1.3 μm wavelength

Cong Wang (王 聪)[1], Qianqian Peng (彭倩倩)[1], Linlin Xin (辛琳琳)[2,*], and Jie Liu (刘 杰)[1,]**

[1]*Shandong Provincial Key Laboratory of Optics and Photonic Device, School of Physics and Electronics, Shandong Normal University, Jinan 250014, China*

[2]*Department of Dermatology, Qianfoshan Hospital of Shandong Province, Jinan 250014, China*

**Corresponding author: xinll158@sina.com; **corresponding author: jieliu@sdnu.edu.cn*

Received October 24, 2018; accepted November 29, 2018; posted online January 24, 2019

Two-dimensional (2D) materials have attracted intense attention in photonics and optoelectronics for their excellent nonlinear characteristics and are applied for the generation of laser pulses. Here, an active–passive Nd:$GdVO_4$ 1.3 μm laser is realized by using an acousto-optic modulator and gold nanobipyramids absorber. The pulse width of 150.5 ns is obtained in the doubly *Q*-switched laser. The compression ratio and enhancement time are 82.6% and 16. The doubly *Q*-switched technology compresses the pulse width, improves the peak power, and stabilizes the pulse, illustrating that double modulation technology opens the door of controllable ultrafast lasers based on 2D materials.

OCIS codes: 140.3070, 140.3380, 140.3480, 140.3540.

doi: 10.3788/COL201917.020003.

A diode-pumped pulse laser for 1.3 μm has been applied to plenty of practical applications, such as remote sensing and air monitoring[1–6]. Actively *Q*-switched technologies and passively *Q*-switched (PQS) technologies are two traditional methods to obtain a pulse laser[7–15]. There are some ways to realize active *Q*-switching such as the acousto-optic modulator (AOM), and saturable absorber (SA) inserted into a resonator can achieve passive *Q*-switching. PQS lasers have the advantages of fast response and simple structure, but the great pulse fluctuation becomes the obstacle of the development of the PQS laser[16]. For active *Q*-switching, it has stable and controllable pulse trains, but the pulse width is wider than the PQS laser[16]. To exert the advantages and avoid the disadvantages of these two technologies, the combination of actively *Q*-switched technologies and PQS technologies, so-called doubly *Q*-switched (DQS) technologies, is achieved. The first DQS technology is obtained by using a spinning mirror and saturable dye[17]. Up to now, the DQS technologies can compress the pulse width, improve the peak power, and obtain a singly symmetric pulse in comparison with singly active or PQS technologies[16,18–24].

DQS technologies at the output wavelength of 940 nm, 1.0 μm, and 2.0 μm have been studied[16,18,21,22,25]. For the wavelength of 1.3 μm, the DQS laser with AOM and V^{3+}-doped yttrium aluminum garnet (V^{3+}:YAG) was reported[23,24]. In 2018, the DQS laser by using Co^{2+}:$MgAl_2O_4$ and AOM was also researched[26]. In recent years, novel SAs extensively promote the development of the pulse laser, including nanometer materials[27–30] and graphene[31,32]. For example, graphene has enabled ultrashort pulse generation in lasers as a passive all-optical modulator for broadband saturable absorption and excellent nonlinear effects. Because of the characteristics of broadband absorption and great third-order nonlinear coefficient (10^{-5}–10^{-6} esu)[33,34], gold nanomaterials are attended. The third-order nonlinear coefficient of gold nanobipyramids (Au-NBPs) is larger than that of graphene. As one of member of gold nanomaterials, the Au-NBPs have a variable surface plasmon resonance (SPR) peak, which can be controlled by the aspects of the materials; the advantage is mainly different from the SAs mentioned in the preceding text[35–38]. Adjusting the extension ratio of Au-NBPs, the response peak will change in the range from the visible region to the near-infrared region. In 2016, the PQS lasers based on the Au-NBPs were reported in the near-infrared region[39–41]. These researches illustrate that the Au-NBPs are a potential SA and can be used for the generation of a pulse laser. However, as far as we know, relevant research is hardly reported about the 1.3 μm DQS laser with AOM and Au-NBPs.

In this Letter, the diode-pumped DQS laser with the AOM and Au-NBPs is first, to the best of our knowledge, realized. The pulse characteristics of singly PQS and DQS lasers are measured. A pulse laser with stable repetition rate and short pulse width is obtained in the DQS laser, suggesting that the pulse qualities are improved relative to the singly PQS laser.

The Au-NBPs were prepared through seed-mediated grown methods, as shown in Fig. 1(a). With regards to the seed solution, 1% $HAuCl_4$ (50 μL) and 1% cirtrate (74 μL) were put into pure water, which was stirred for 1 min. Then, 0.01 M (1 M = 1 mol/L) ice $NaBH_4$ (150 μL) was dropped into the seed solution, which was stirred for 1 min. For the grown solution, cetyltributylammonium bromide (0.01 M, 28.5 mL), gold chloride acid (0.01 M, 1.2 mL), $AgNO_3$ (0.01 M, 60 μL), and 0.1 M

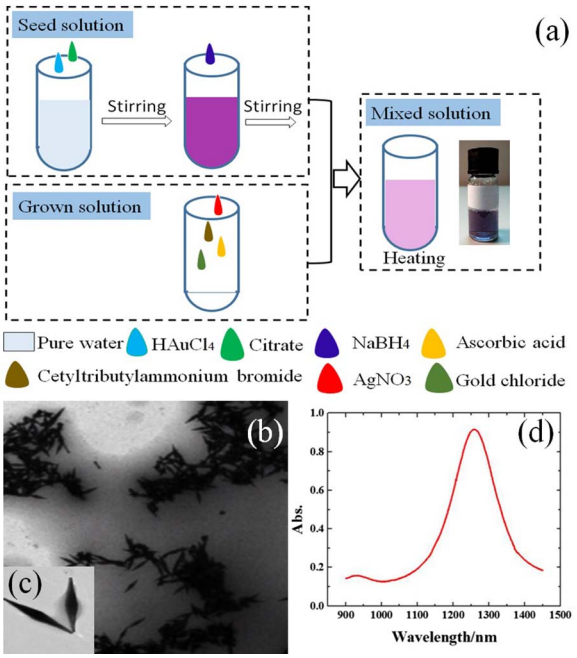

Fig. 1. (a) Fabrication process of Au-NBPs. TEM image with a scale of (b) 2000 nm and (c) 100 nm. (d) Absorption spectrum of Au-NBPs.

ascorbic acid (0.4 mL) were mixed. Finally, the seed solution (30 μL) was added into the grown solution. The mixed solution was heated in an oven maintained at 65°C for 10 h to get Au-NBPs. The transmission electron microscope (TEM) images of the Au-NBPs are depicted in Figs. 1(b) and 1(c), suggesting that the Au-NBPs were successfully fabricated. The absorption peak of the Au-NBPs is located at the wavelength of 1260 nm, as shown in Fig. 1(d).

We established a V-shaped folded cavity with a length of 203 mm to generate short pulse lasers, as shown in Fig. 2. Simulating the spot radius by the ABCD matrix in the gain medium and SA close to the output coupling, the radius is estimated to be 210 and 100 μm, respectively. The cavity design is beneficial to weakening the thermal lens effect and improving the pattern matching. The V-shaped folded cavity consists of M1 ($R = \infty$), M2 ($R = 100$ mm), and M3 ($R = \infty$) gain media. The plane mirror M1 and the concave mirror M2 have high-reflection (HR) coating for 1342 nm. M2 has high-transmittance (HT) coating for 808 nm. The plane mirror M3 with 4% transmittance for 1342 nm acts as the output coupler.

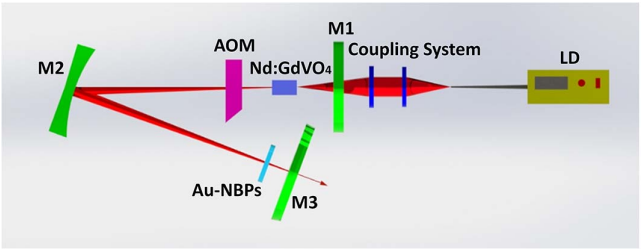

Fig. 2. Experimental setup of DQS Nd:$GdVO_4$ laser.

Nd:$GdVO_4$ acts as the gain medium. The size of Nd:$GdVO_4$ is 4 mm × 4 mm × 9 mm, and the two end surfaces of the gain medium have anti-reflection (AR) coating for 808 and 1342 nm. The Nd:$GdVO_4$ is wrapped by silver foil mounted at a copper block. A water cooler maintained at 15°C was used to move the heat. It was pumped by a fiber-coupled laser diode with a center wavelength of 808 nm to improve conversion efficiency. The beam was collimated to reduce dispersion and then focused on the gain medium by a coupling system of 1:1; there was a spot of 200 μm on the Nd:$GdVO_4$. The AOM (26th Institution, CETC, China) and the Au-NBPs acted as the active element and SA, respectively. The nonlinear curve of the adopted Au-NBPs (the modulation depth of 10% and saturable optical intensity of 750 mW/cm^2) has been reported in our previous work[41]. The output laser was measured by a digital oscilloscope (Tektronix DPO 4104, USA).

Firstly, we carefully adjusted the cavity to obtain maximum continuous wave power, insuring that the V-shaped cavity kept optimum conditions. Then, after inserting the near-infrared quartz plate coated with Au-NBPs, a singly PQS laser is realized by finely tuning the position of the quartz plate. In Fig. 3, it shows pulse characteristics as a function of the absorbed pump power. Under the absorbed pump power of 4.2 W, the maximum average output power is 160 mW, as shown in Fig. 3(a). The pulse is stable in the absorbed pump power ranging from 2.9 to 4.1 W. In Fig. 3(b), the pulse width decreases with the augmentation of the absorbed pump power. The shortest pulse duration is 862 ns, namely, the repetition rate is 74.5 kHz. The pulse width of several hundred nanoseconds can be attributed to the long cavity length. If the absorbed pump power is further increased, the pulse will become unstable. Therefore, we reduce the absorbed pump power to zero to protect the Au-NBPs. Repeating this experiment again (from 2.9 to 4.1 W), the stable Q-switched laser is still obtained. It suggests that the Au-NBPs are not damaged.

After finishing the PQS laser, the DQS laser is realized by inserting the AOM. Figure 4 depicts pulse characteristics as functions of the absorbed pump power. It is clear that the output power of 97 mW and the laser threshold of 2.7 W are obtained at the modulation frequency of 30 kHz, as shown in Fig. 4(a). Compared with the PQS laser,

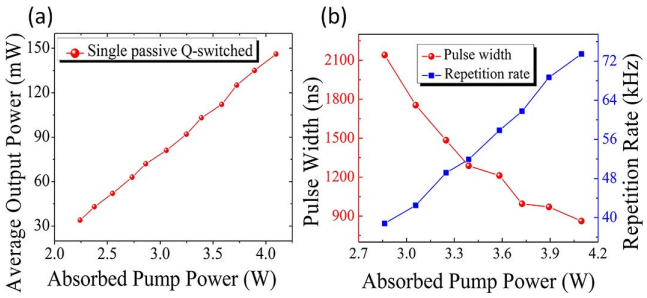

Fig. 3. (a) Average output power and (b) pulse width and repetition rate versus absorbed pump power.

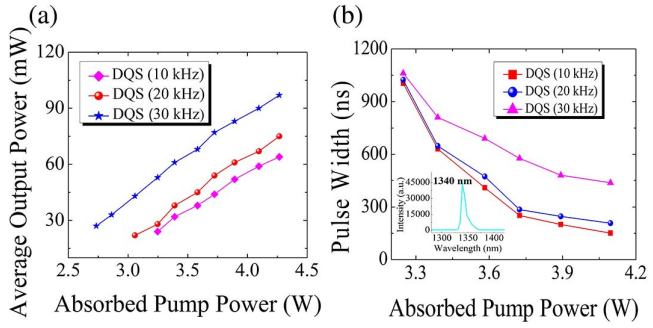

Fig. 4. (a) Average output power and (b) pulse width versus absorbed pump power at the DQS laser. Inset, output spectrum.

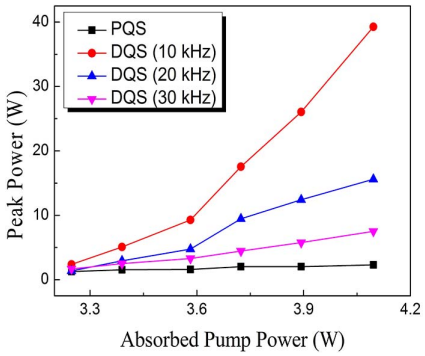

Fig. 5. Peak power versus absorbed pump power.

the DQS laser has a lower output power and a higher threshold. This phenomenon results from the insertion of the AOM, leading to more losses. The lasers operate at 1.3 μm, as depicted in the inset of Fig. 3(b). In Fig. 4(b), the shortest pulse duration is 150.5 ns in the DQS laser at the modulation frequency of 10 kHz. The obtained pulse width is shorter than in the previous work using the same SA[41]. Obviously, the pulse width is generally compressed in the DQS laser. At the low modulation frequency, the intracavity population has a longer time to accumulate, leading a shorter laser pulse being obtained. So, the pulse width becomes wider with the increase of the modulation frequency of the AOM. Peak power is also another important parameter for laser pulses, which can be calculated by the known parameters. In Fig. 5, the calculated peak power is depicted for the PQS and DQS lasers. Obviously, the peak power is improved in the dual-loss modulation. Under the condition of the absorbed pump power of 4.1 W and the modulation frequency of 10 kHz, the peak power is 39.2 W.

As mentioned above, the pulse width is compressed in the DQS laser when compared with the single PQS laser. In order to describe the degree of the narrowing of the pulse width, a compression ratio t_c is defined as $t_c = (t_s - t_d)/t_s$, where t_s and t_d are the pulse duration of the PQS and DQS lasers, respectively. Table 1 shows

Table 1. Compression Ratio and Enhancement Time at Different Modulation Frequencies of DQS Laser

	DQS laser		
	10 kHz	20 kHz	30 kHz
Compression ratio	82.6%	75.1%	53.6%
Enhancement time	16.0	5.8	2.3

the compression ratio t_c at different acousto-optic modulation frequencies of the DQS laser under the same absorbed pump power. The maximum compression ratio of 82.6% is obtained under the modulation frequency of 10 kHz. An enhancement time P_i is defined to illustrate the improvement of peak power in the DQS laser. $P_i = (P_d - P_s)/P_s$, where P_d and P_s are the peak power of the DQS and PQS lasers, respectively. In Table 1, the enhancement times at the different modulation frequencies are shown at the absorbed pump power of 4.1 W. The maximum enhancement time is 16 at the modulation frequency of 10 kHz.

The pulse profiles and pulse trains for PQS and DQS lasers are demonstrated in Fig. 6. The obtained pulse widths of PQS and DQS lasers (74.5, 10, 20, and 30 kHz) are

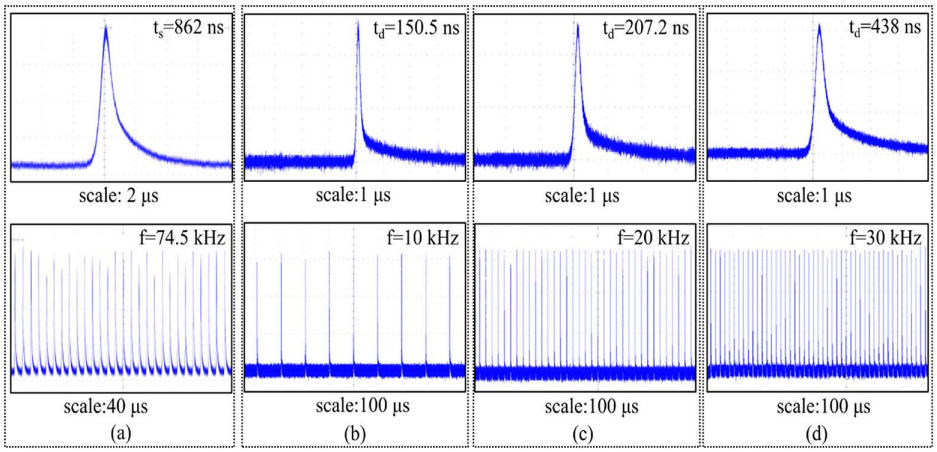

Fig. 6. Temporal pulse profiles and pulse trains for (a) singly PQS laser and DQS laser at the modulation frequencies of (b) 10 kHz, (c) 20 kHz, and (d) 30 kHz.

862, 150.5, 207.2, and 438 ns, respectively. We know that the pulse width is directly proportional to the cavity time constant τ_c according to $\tau_c = 2L/c(T+\delta)$[18], where T is the transmission of output coupler, δ is the round-trip loss, and L and c represent the cavity length and the speed of light, respectively. The inserted Au-NBPs lead to an extra loss to shorten the pulse width in the DQS laser. In Fig. 6(a), the pulse fluctuation is 10.6%, indicating the pulse is not fully stable. The pulse trains are stable [Figs. 6(b), 6(c), and 6(d)], and the repetition rate is equal to the modulation frequency of the AOM. The phenomenon is related to the time of the buildup of a pulse. The pulse repetition rate of passive Q-switching is about 74.5 kHz, which indicates that a single laser pulse takes 13 μs to establish. For double Q-switching, the modulation frequency of the AOM (10, 20, and 30 kHz) is smaller than the repetition rate of passive Q-switching. The buildup of a pulse needs more time to generate in the DQS laser. Thus, the repetition rate of the double Q-switching corresponds with the modulation frequency of the AOM.

In conclusion, the Nd:$GdVO_4$ 1.3 μm laser is first, to the best of our knowledge, achieved by using the AOM and Au-NBPs. The pulse width is shorter, the peak power is greater, and the pulse is more stable in the DQS laser. Moreover, the compression ratio and the enhancement time are 82.6% and 16. The DQS technologies have a good advantage of application in ultrafast lasers due to their short pulse width, high peak power, and controllable repetition rate. If the 2D materials and cavity are further optimized, the pulse characteristics will be better.

This work was supported by the National Natural Science Foundation of China (No. 61475089) and the Development Projects of Shandong Province Science and Technology (No. 2017GGX30102).

References

1. U. Keller, J. A. Valdmanis, M. C. Nuss, and A. M. Johnson, IEEE J. Quantum Electron. **24**, 427 (1988).
2. R. Fluck, G. Zhang, U. Keller, K. J. Weingarten, and M. Moser, Opt. Lett. **21**, 1378 (1993).
3. K. W. Su, H. C. Lai, A. Li, Y. F. Chen, and K. E. Huang, Opt. Lett. **30**, 1482 (2005).
4. V. Liverini, S. Schön, R. Grange, M. Haiml, S. C. Zeller, and U. Keller, Appl. Phys. Lett. **84**, 4002 (2004).
5. J. Xu, Y. Yang, J. He, B. Zhang, X. Yang, S. Liu, B. Zhang, and H. Yang, IEEE J. Quantum Electron. **48**, 622 (2012).
6. W. Cai, S. Jiang, S. Xu, Y. Li, J. Liu, C. Li, L. Zheng, L. Su, and J. Xu, Opt. Laser Technol. **65**, 1 (2015).
7. F. Zhang, J. Liu, W. Li, B. Mei, D. Jiang, X. Qian, and L. Su, Opt. Eng. **55**, 106114 (2016).
8. L. J. Li, B. Q. Yao, C. W. Song, Y. Z. Wang, and Z. G. Wang, Laser Phys. Lett. **6**, 102 (2009).
9. A. F. El-Sherif and T. A. King, Opt. Commun. **218**, 337 (2003).
10. C. Li, M. Fan, J. Liu, L. Su, D. Jiang, X. Qian, and J. Xu, Opt. Laser Technol. **69**, 140 (2015).
11. Y. Wu, C. Zhang, J. Liu, H. Zhang, J. Yang, and J. Liu, Opt. Laser Technol. **97**, 268 (2017).
12. Y. Zhao, Z. Wang, H. Yu, L. Guo, L. Chen, S. Zhuang, X. Sun, D. H. Hu, and X. Xu, Chin. Opt. Lett. **9**, 081401 (2011).
13. M. Lin, Q. Peng, W. Hou, X. Fan, and J. Liu, Opt. Laser Technol. **109**, 90 (2019).
14. J. Ma, S. B. Lu, Z. N. Guo, X. D. Xu, H. Zhang, D. Y. Tang, and D. Y. Fan, Opt. Express **23**, 22643 (2015).
15. J. Li, H. Luo, B. Zhai, R. Lu, Z. Guo, H. Zhang, and Y. Liu, Sci. Rep. **6**, 30361 (2016).
16. C. Luan, K. Yang, J. Zhao, S. Zhao, W. Qiao, T. Li, C. Liu, H. Chu, J. Qiao, L. Zheng, X. Xu, and J. Xu, Laser Phys. Lett. **13**, 025006 (2016).
17. D. Hull, Appl. Opt. **5**, 1342 (1966).
18. C. Luan, K. J. Yang, J. Zhao, S. Z. Zhao, W. C. Qiao, T. Li, T. L. Feng, C. Liu, J. P. Qiao, L. H. Zheng, J. Xu, Q. G. Wang, and L. B. Su, Appl. Opt. **54**, 8024 (2015).
19. T. W. Chen, K. C. Chang, J. C. Chen, J. H. Lin, and M. D. Wei, Appl. Opt. **53**, 3459 (2014).
20. D. Wang, J. Zhao, K. Yang, S. Zhao, T. Li, D. Li, G. Li, and W. Qiao, Opt. Mater. **72**, 464 (2017).
21. G. Q. Li, S. Z. Zhao, K. J. Yang, and W. Wu, Jpn. J. Appl. Phys. **44**, 3017 (2005).
22. B. Zhao, Y. Chen, B. Yao, Z. Cui, S. Bai, H. Yang, X. Duan, J. Li, Y. Shen, C. Qian, J. Yuan, T. Dai, C. Li, and Y. Pan, Opt. Eng. **55**, 116116 (2016).
23. Y. Li, S. Zhao, C. Feng, and K. Cheng, Laser Phys. **22**, 693 (2012).
24. D. Wang, J. Zhao, K. Yang, S. Zhao, T. Li, D. Li, G. Li, and W. Qiao, Opt. Quantum Electron. **48**, 553 (2016).
25. B. Bai, Y. Bai, D. Li, Y. Sun, J. Li, and J. Bai, Chin. Opt. Lett. **16**, 031402 (2018).
26. C. Wang, J. Liu, Y. Zu, X. Fan, and J. Liu, Opt. Quantum Electron. **50**, 122 (2018).
27. C. Zhang, J. Liu, X. Fan, Q. Peng, X. Guo, D. Jiang, X. Qian, and L. Su, Opt. Laser Technol. **103**, 89 (2018).
28. J. Liu, Y. Wang, Z. Qu, and X. Fan, Opt. Laser Technol. **44**, 960 (2012).
29. Y. Xue, Z. D. Xie, Z. L. Ye, X. P. Hu, J. L. Xu, and H. Zhang, Chin. Opt. Lett. **16**, 020018 (2018).
30. H. Mu, Z. Wang, J. Yuan, S. Xiao, C. Chen, Y. Chen, Y. Chen, J. Song, Y. Wang, Y. Xue, H. Zhang, and Q. Bao, ACS Photon. **2**, 832 (2015).
31. H. Wan, W. Cai, F. Wang, S. Jiang, S. Xu, and J. Liu, Opt. Quantum Electron. **48**, 11 (2015).
32. M. N. Cizmeciyan, J. W. Kim, S. Bae, B. H. Hong, F. Rotermund, and A. Sennaroglu, Opt. Lett. **38**, 341 (2013).
33. H. B. Liao, R. F. Xiao, J. S. Fu, P. Yu, G. K. L. Wong, and P. Sheng, Appl. Phys. Lett. **70**, 1 (1997).
34. S. Yamashita, J. Lightwave Technol. **30**, 427 (2012).
35. Z. Kang, Y. Xu, L. Zhang, Z. Jia, L. Liu, D. Zhao, Y. Feng, G. Qin, and W. Qin, Appl. Phys. Lett. **103**, 041105 (2013).
36. T. Jiang, Y. Xu, Q. Tian, L. Liu, Z. Kang, R. Yang, G. Qin, and W. Qin, Appl. Phys. Lett. **101**, 151122 (2012).
37. Z. Kang, Q. Li, X. J. Gao, L. Zhang, Z. X. Jia, Y. Feng, G. S. Qin, and W. P. Qin, Laser Phys. Lett. **11**, 035102 (2014).
38. D. Fan, C. Mou, X. Bai, S. Wang, N. Chen, and X. Zeng, Opt. Express **22**, 18537 (2014).
39. H. Zhang and J. Liu, Opt. Lett. **41**, 1150 (2016).
40. H. Zhang, B. Li, and J. Liu, Appl. Opt. **55**, 7351 (2016).
41. Z. Chu, H. Zhang, Y. Wu, C. Zhang, J. Liu, and J. Yang, Opt. Commun. **406**, 209 (2018).